



Thermal behavior and kinetic study on the pyrolysis of lean coal blends with thermally dissolved coal

Longfei Guo¹ · Haibin Zuo¹  · Yajie Wang¹ · Jun Zhao¹

Received: 27 May 2018 / Accepted: 28 August 2018 / Published online: 7 September 2018
© Akadémiai Kiadó, Budapest, Hungary 2018

Abstract

In this paper, we use organic solvent *N*-methyl pyrrolidone (NMP) to thermally dissolve Kelan (KL) coal. The final product is thermally dissolved coal (TDC). The thermal behavior and non-isothermal kinetics of Guandi (GD) coal and TDC, as well as the co-pyrolysis of coal blends, have been studied by three methods (Friedman method (FR), Flynn–Wall–Ozawa method (FWO) and distributed activation energy model (DAEM)). Obtained results show that TDC has a higher maximum devolatilization rate and lower temperature corresponding to the starting and maximum rates of pyrolysis, compared to GD coal. The addition of TDC not only improves the maximum devolatilization rate of coal blends, but also reduces the temperature corresponding to the maximum devolatilization rate. Obtained results indicate that synergistic reactions may occur between the temperatures corresponding to the maximum devolatilization rates of GD and TDC. In this study, the apparent activation energy E obtained by FR, FWO and DAEM methods of coal blends with various addition of TDC almost increased with increasing conversion. There is a kinetic compensation effect in the kinetic process of coal pyrolysis and the reaction kinetics compensation effect equation.

Keywords Thermally dissolved coal · Pyrolysis · Thermal behavior · Kinetics

Introduction

As a traditional fuel source, low-rank coals are widely used in China [1, 2] Meanwhile, coal fines as a by-product are inevitably produced during mining, transportation and production of low-rank coal [3]. Using coal fines as raw material to produce coal briquettes is of great practical significance in improving their value and protecting environment [4]. However, the addition of binders in the production of coal briquettes may increase the amount of ash in the coal. The thermal dissolution of coal using organic solvents has become an efficient method of coal utilization [5]. Thermally dissolved coals are characterized by low-ash or ash-free, high volatile content and high thermal plasticity [6, 7]. Chang et al. proposed an ash-free coal extracted as an additive or alternative for coal blends [8]. Coal blends exhibit significant improvements in their

properties, such as caking and strength of the coal [9]. Therefore, thermally dissolved coals can enhance the process of coal briquette production.

Coal pyrolysis is the preliminary conversion processes of coal resources, such as carbonization, gasification and combustion [10, 11]. It is crucial that study the pyrolysis of coal blends to detect the effect of additives on this process and to uncover the possible mechanism of synergistic reactions. In order to obtain the relevant kinetic parameters of coal pyrolysis, two methods of data processing, derived from non-isothermal thermogravimetric analysis, can be utilized, namely the ‘model-free’ and ‘model-fitting’ methods, respectively [12–15]. However, the model-fitting method inevitably has two main deficiencies. Firstly, because of the so-called kinetic compensation effect [16], the same thermogravimetric curve can be described by different models with different values of kinetic parameters, especially when the data are solely derived from a single heating rate, resulting in an ambiguous interpretation of the results. Applying data obtained from multiple heating rates can effectively eliminate this effect. It is generally considered that the kinetic parameters obtained from the

✉ Haibin Zuo
zuohaibin@ustb.edu.cn

¹ State Key Laboratory of Advanced Metallurgy, University of Science and Technology Beijing, Beijing 100083, China

model-fitting method correspond to the whole range of conversion. However, the previous study showed that the activation energy of coal pyrolysis is varied with conversion to take the place of a constant during the action. In contrast, the model-free methods do not require the specific pyrolysis model $f(\alpha)$. For the main model-free methods, the iso-conversional methods always hold the assumption of E as a function of conversion based on data from multiple heating rates and are gradually applied in studies on the kinetics of coal thermochemical conversion. Distributed activation energy model (DAEM) [17] method using infinite parallel first-order reaction assumptions in a wide range of temperatures and heating rate of the reaction processes accurately describes the solid-phase reaction, including the process of coal pyrolysis.

This work investigates the thermal behavior and kinetics of both a typical lean coal and a thermally dissolved coal, as well as those of coal blends with different ratios of thermally dissolved coal. The effects of heating rate and additive volume of thermally dissolved coal on the pyrolysis process were studied. By comparing the difference between the pyrolysis process of individual coal sample and mixed coal sample, the temperature range of synergistic reaction was identified. We also investigated the kinetic compensation effect in pyrolysis of coal. It is expected that this study will be useful to comprehensively understand the pyrolysis process of coal and effectively provide the information for the design and operation of the reactor.

Experimental

Sample preparation

Two common types of Chinese coals, namely Guandi (GD) and Kelan (KL) coal, were selected for this study. GD coal is a lean coal which does not have cohesiveness and have limited applications. KL coal is a gas coal with a relatively high volatile content. After dried at 105 °C for 10 h, GD and KL coal samples were ground and sieved to a particle size less than 0.074 mm. The milled GD coal was prepared for the subsequent pyrolysis process. The milled KL coal was prepared for the thermal extraction process, and the procedure is detailed below.

The extracted KL coal was thermally prepared in an autoclave using a recyclable organic solvent (*N*-methyl pyrrolidone, NMP). The pre-dried KL coal (8 g) and NMP (400 mL) were placed in an autoclave reactor. Firstly, the reactor was purged with N₂ at a rate of 400 mL min⁻¹, for 20 min. After the air was removed, the air inlet and outlet were closed and the pressure in the autoclave was equal to the atmospheric pressure. Thermal extraction was

performed under nitrogen atmosphere, at 350 °C for 1 h. To fully promote the mixture of the pulverized coal and the organic solvent, the mixture was stirred at a speed of 100 rad min⁻¹ during the experiment. After the experiment, the designed temperature program was terminated and the heating mantle was removed to air-cool the contents to room temperature. The extract was filtered using a Buchner funnel and filter paper to obtain the liquid phase and the residue, respectively. Then, the intermediate product was separated by vacuum rotary evaporator from the liquid above mentioned and the residual liquid (the organic solvent) was recycled in the next extraction. The solid product was repeatedly rinsed with alcohol and deionized water and then dried under vacuum at 80 °C for 12 h. The final product, named thermally dissolved coal (TDC), was ground and sieved to a particle size less than 0.074 mm. The results of the proximate, ultimate analysis and calorific value of the GD, TDC and KL coal samples are presented in Table 1. The calorific values of all samples are based on the paper of Parikh [18].

Pyrolysis process

Pyrolysis experiments of coal samples were performed using a thermogravimetric analyzer (NETZSCH, STA 449 F3, Germany) with high loading capacity (35,000 mg) and sensitivity (0.1 µg). According to previous literature, approximately 10 mg of coal sample was placed in a ceramic crucible (height: 2 mm; circular base diameter: 5 mm), to ignore the limitations of the external and intra-particle heat transfer [19, 20]. In this work, all tests were performed from room temperature to 1000 °C at three different heating rates: 10 °C min⁻¹, 20 °C min⁻¹ and 30 °C min⁻¹. For the pyrolysis of coal blends, GD-TDC blends were prepared according to the following mix ratios (by mass): 90:10, 80:20 and 70:30, respectively. Firstly, samples were placed at 50 °C for 10 min to remove air. During pyrolysis, high purity argon was added at rate of 100 mL min⁻¹ to ensure the inert atmosphere around the sample [21]. The signal of sample residual mass and temperature over time was recorded automatically by the TG device.

Kinetic analysis

For the kinetic analysis of coal pyrolysis, it is usually assumed that the rates of conversion are proportional to the concentration of reacted material. The reaction rate of coal pyrolysis can be described as follows:

$$\frac{d\alpha}{dt} = k(T)f(\alpha) = A \exp\left(\frac{-E}{RT}\right)f(\alpha) \quad (1)$$

where α is the extent of conversion, t is the pyrolysis time, $k(T)$ is the Arrhenius rate constant, A and E are the

Table 1 Proximate and ultimate analysis of coal samples

Sample	Proximate analysis/mass%			Ultimate analysis/mass%					Calorific value/MJ kg ⁻¹
	V	A	FC	C	H	N	S	O ^b	
GD ^a	14.31	9.14	76.55	80.19	3.78	1.23	1.22	3.65	29.37
TDC ^a	49.91	0.49	50.00	79.13	5.27	4.14	0.53	6.85	25.46
KL ^a	32.20	10.37	55.43	73.38	4.73	1.59	0.96	7.48	24.70

^aOn the dry basis (d)^bBy difference

preexponential factor and activation energy, respectively, R is the gas constant, T is the temperature and $f(\alpha)$ is the kinetic model-dependent function. The conversion, α , is derived from the equation $\alpha = (m_0 - m)/(m_0 - m_f)$ where m_0 and m_f are the initial and final mass, respectively, in the non-isothermal temperature range used for this study (100–1000 °C). In this paper, pyrolysis was studied using the linear heating program:

$$\frac{dT(t)}{dt} = \beta \quad (2)$$

where β is the heating rate.

Therefore, under non-isothermal and heterogeneous conditions, the kinetic equation of coal pyrolysis is transformed into the following expression:

$$\frac{d\alpha}{dT} = \frac{A}{\beta} \exp\left(\frac{-E}{RT}\right) f(\alpha) \quad (3)$$

Friedman method (FR) [22]

The model-free or iso-conversional methods do not require a specific pyrolysis model $f(\alpha)$, but only a simple transformation of the formula with some approximations.

By taking the logarithm of the two sides of Eq. (3), it can be directly obtained the following formula whose logarithm is

$$\ln\left(\beta \frac{d\alpha}{dT}\right) = \ln[Af(\alpha)] - \frac{E}{RT} \quad (4)$$

In which FR is a differential iso-conversional method. From this equation, it is easy to obtain values for E over a wide range of conversions, by plotting $\ln\left(\beta \frac{d\alpha}{dT}\right)$ against $\frac{1}{T}$, for a constant α value.

Flynn–Wall–Ozawa method (FWO) [23, 24]

The basic Eq. (3) can also be shown as follows:

$$\frac{d\alpha}{f(\alpha)} = \frac{A}{\beta} \exp\left(\frac{-E}{RT}\right) dT \quad (5)$$

By defining a new function $g(\alpha)$, it is easy to obtain the following expression:

$$g(\alpha) = \int_0^\alpha \frac{d\alpha}{f(\alpha)} = \frac{A}{\beta} \int_{T_0}^T \exp\left(\frac{-E}{RT}\right) dT = \frac{AE}{\beta R} p(\mu) \quad (6)$$

where $p(\mu) = \int_\infty^\mu \frac{e^{-\mu}}{\mu^2} d\mu$, $\mu = \frac{E}{RT}$.

Then Eq. (6) can be integrated to give the following equation in logarithmic form:

$$\ln g(\alpha) = \ln \frac{AE}{R} - \ln \beta + \ln p(\mu) \quad (7)$$

Since the integral $p(\mu)$ has no analytical solution, only the numerical solution, using Doyle's approximation [25] for the integral which allows $(\ln p(\mu) \cong -5.331 - 1.052 \frac{E}{RT})$ for FWO method. Equation (7) now can be simplified as

$$\ln \beta = \ln \frac{AE}{Rg(\alpha)} - 5.331 - 1.052 \frac{E}{RT} \quad (8)$$

Thus, for $\alpha = \text{constant}$, the plot $\ln \beta$ vs. $\frac{1}{T}$ should be a straight line whose slope can be used to evaluate the activation energy (E).

Distributed activation energy model (DAEM)

The distributed activation energy model (DAEM) was established to clearly describe the complex chemical reactions, which has a good ability on the determination of the kinetic parameters for a series of parallel reactions with different values of activation energy. The common expression is as follows

$$\ln\left(\frac{\beta}{T^2}\right) = \ln\left(\frac{AR}{E}\right) + 0.6075 - \frac{E}{RT} \quad (9)$$

From the intercept and slope of this equation, it is easy to obtain values for E and A .

Results and discussion

Thermal behavior

Thermal behavior of individual coal samples

Figure 1 shows the mass (TG) and derivative of mass (DTG) curves of pyrolysis under non-isothermal conditions, for single samples of GD coal and TDC, at $20\text{ }^{\circ}\text{C min}^{-1}$, under inert atmosphere. The TG curve represents the percentage of residual sample mass from the initial sample mass, and the DTG curve represents the mass loss rate due to devolatilization during pyrolysis. In Fig. 1a, the thick red line indicates the heating process at $20\text{ }^{\circ}\text{C min}^{-1}$. Because the model described in Sect. 2.3 is based on non-isothermal kinetics with a constant heating rate, all subsequent analysis is focused on the temperature range corresponding to the non-isothermal region of the plot, as depicted in Fig. 1a. Consequently, all following results are based on the temperature range from 100 to $1000\text{ }^{\circ}\text{C}$.

During the devolatilization process, significant mass loss of TDC started at approximately $200\text{ }^{\circ}\text{C}$, which was significantly lower than the temperature corresponding to the start of GD coal devolatilization (approximately $400\text{ }^{\circ}\text{C}$). The maximum devolatilization rate of TDC ($3.32\% \text{ min}^{-1}$) shown in the DTG curves (Fig. 1b) is almost three times the maximum mass loss rate of GD coal ($1.14\% \text{ min}^{-1}$). Rapid mass loss in the GD coal occurred in a narrower temperature range (approximately $400\text{--}900\text{ }^{\circ}\text{C}$) than that of TDC (approximately $200\text{--}900\text{ }^{\circ}\text{C}$). As indicated by the higher devolatilization rate and wider temperature range with rapid mass loss rate, the total volatile content of TDC (38.18 mass%) is greater than that of GD coal (13.82 mass%).

The DTG curves of the GD coal and TDC at different heating rates are shown in Fig. 2. The heating rate has a

similar effect on all DTG curves which is independent of coal type. When the heating rate increases, the maximum devolatilization rate also increases and the temperature corresponding to the maximum devolatilization rate is shifted to the high-temperature zone. This is due to the occurrence of thermal lag as the heating rate increases, which is consistent with previously reported results [21]. The detailed characteristic information of the DTG curves is shown in Table 2. The incremental percentage of the maximum devolatilization rate of GD coal (3.01%) is greater than that of TDC (1.04%), which indicates that the heating rate has a greater influence on GD coal than on TDC. The maximum reaction rate of GD coal occurs at about 0.31 conversion, while that of TDC occurs at about 0.52 conversion.

Thermal behavior of mixed coal samples

Figure 3 shows the TG and DTG curves of GD-TDC with various mix ratios, obtained at $20\text{ }^{\circ}\text{C min}^{-1}$. There are similar variations in TG and DTG curves at specific mix ratios. The mass loss of blends increases with the increase in the amount of TDC, due to its high volatile content. Based on the DTG curves of blends, addition of TDC not only improves the maximum devolatilization rate of blends, but also reduces its corresponding temperature. The DTG curve of the mixture with high TDC content almost completely covers the DTG curve of the blend with low TDC. The improvement in the maximum devolatilization rate of coal blends occurred mainly at temperature lower than $550\text{ }^{\circ}\text{C}$, which is similar to the temperature corresponding to the maximum devolatilization rate of GD coal. This is mainly due to that the difference in devolatilization rate between GD coal and TDC becomes smaller after $550\text{ }^{\circ}\text{C}$. Figure 4 also shows the DTG curves GD-TDC blends with various mix ratios, obtained at $20\text{ }^{\circ}\text{C min}^{-1}$,

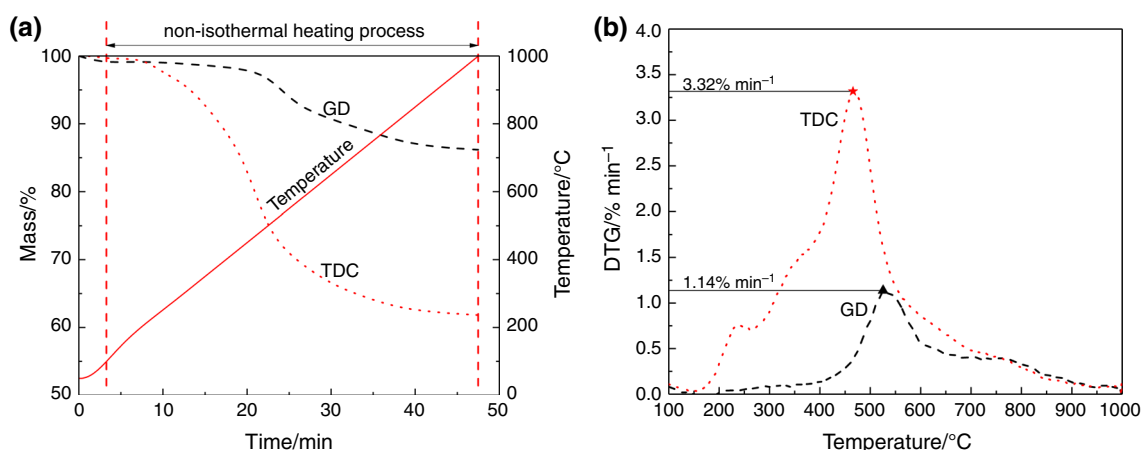


Fig. 1 Mass (TG) and derivative of mass (DTG) curves of individual sample pyrolysis at $20\text{ }^{\circ}\text{C min}^{-1}$

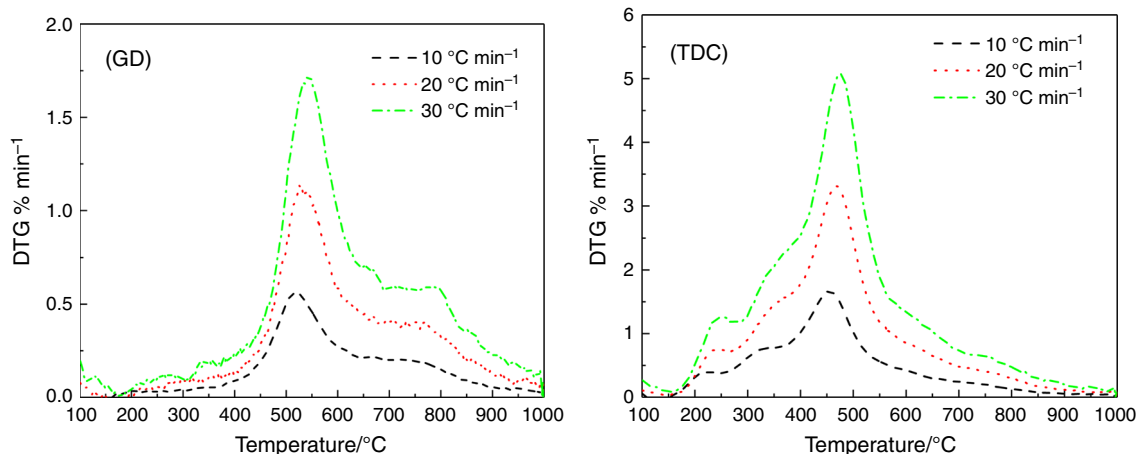


Fig. 2 DTG curves of GD coal and TDC at different heating rates

Table 2 Devolatilization parameters of GD coal and TDC at different heating rates

Sample	Heating rate/ $^{\circ}\text{C min}^{-1}$	$T_m/^{\circ}\text{C}$	Conversion	$(d\alpha/dt)_m/\% \text{ min}^{-1}$	$(d\alpha/dT)_m/\% \text{ }^{\circ}\text{C}^{-1}$	$\Delta(d\alpha/dT)_m/\%$
GD	10	518.75	0.31	0.56	1.68	3.01%
	20	525.42	0.31	1.14	1.70	
	30	543.38	0.32	1.73	1.73	
TDC	10	454.09	0.52	1.67	5.01	1.41%
	20	465.72	0.51	3.32	4.98	
	30	474.22	0.52	5.08	5.08	

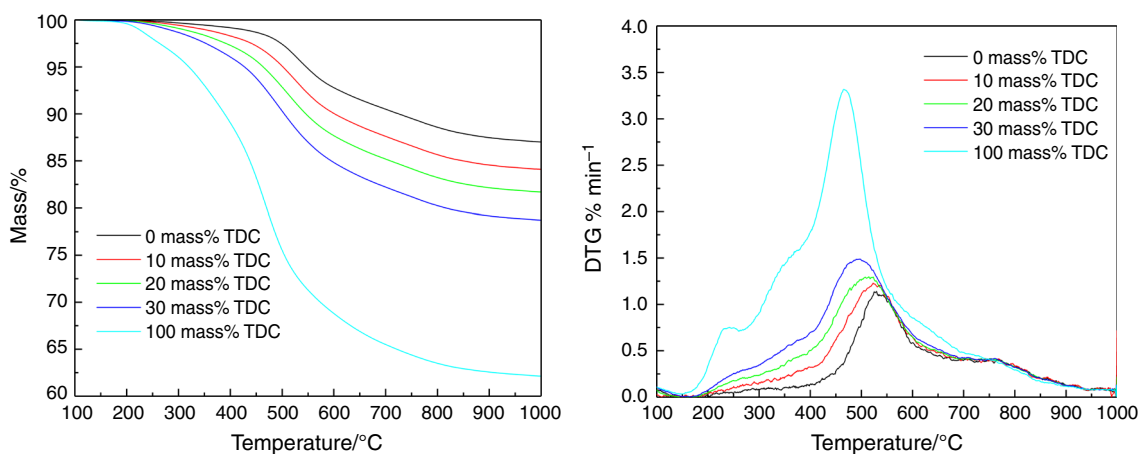


Fig. 3 TD and DTG curves of GD-TDC blends with various mix ratios, obtained at $20 \text{ }^{\circ}\text{C min}^{-1}$

and the detailed information is shown in Table 3. With the increasing amount of TDC, the conversion corresponding to the maximum reaction rate of blends increased from 0.30 to 0.51, which indicates that the maximum reaction of blends occurred later than that of single GD coal. Therefore, the maximum pyrolysis rate of GD-TDC blends was a function of the relative contribution of each sample to the blends, which means that relative contribution of each

sample contribution can be derived by mathematical deconvolution.

Figure 5 shows the influence of the different percentages of TDC on final volatile yields. The experimental value for all samples is the average of 10, 20 and $30 \text{ }^{\circ}\text{C min}^{-1}$, at $1000 \text{ }^{\circ}\text{C}$. The calculated volatile yield of the coal blends is based on the following equation:

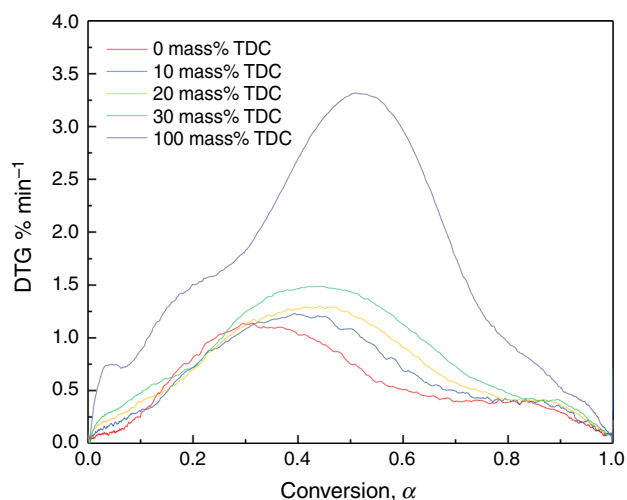


Fig. 4 DTG curves of GD-TDC blends with various mix ratios, obtained at 20 °C min^{-1}

Table 3 Devolatilization parameters of coal blends at 20 °C min^{-1}

mass% TDC	$T_m/\text{°C}$	Conversion _m	$(dx/dt)_m/\text{°C min}^{-1}$
0	525.42	0.30	1.14
10	522.87	0.39	1.23
20	514.49	0.44	1.30
30	497.12	0.45	1.49
100	465.72	0.51	3.32

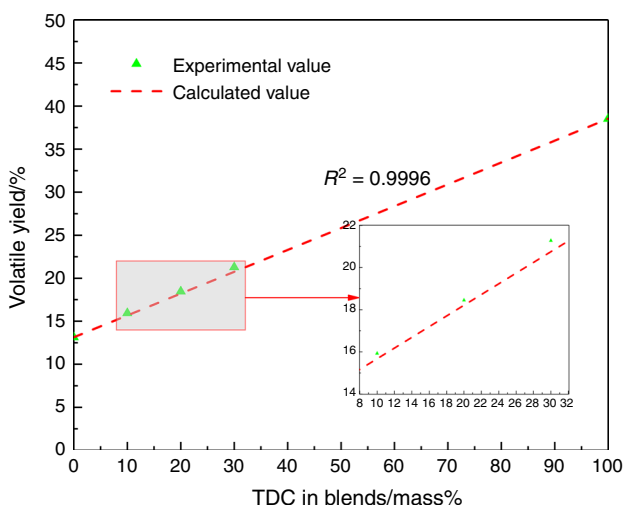


Fig. 5 Influence of content of TDC on final volatile yields (plotted data represent the average of 10, 20 and 30 °C min^{-1} , at 1000 °C)

$$Y = X_{\text{GD}}Y_{\text{GD}} + X_{\text{TDC}}Y_{\text{TDC}} \quad (10)$$

where Y is the calculated volatile yield of the blend, X_{GD} is the fraction of GD coal in the blend sample, X_{TDC} is the fraction of TDC in the blend sample, Y_{GD} is the

experimental volatile yield of single GD coal, and Y_{TDC} is the experimental volatile yield of single TDC.

In order to determine the possible synergistic reactions between GD coal and TDC, the experimental and calculated mass loss and mass loss rate of blends are compared in Fig. 6, which shows the difference between the experimental and calculated TG and DTG curves of blends with 30 mass% TDC at 10 °C min^{-1} . If there is no synergy between the two samples, the experimental values (the circle in Fig. 6) should be located on the line (the calculated values). As can be seen from Fig. 6, there is a gap between the experimental and calculated values. Calculated curves were based on weighted average of the contributing fractions, as detailed in Eq. (5). As the TG curves of coal blends show, the experimental and calculated values were closely match when the temperature was below 450 °C , which means that there are no synergistic reactions up to this temperature. The gap between the experimental and calculated TG curves of coal blends increases when the temperature rises. However, the gap between the experimental and calculated DTG curves of blends lasted until about 520 °C . In addition, 450 °C and 520 °C are similar to the temperatures corresponding to the maximum devolatilization rates of GD coal and TDC, respectively. This indicates that there may exist synergistic reactions between the temperatures corresponding to the maximum devolatilization rates of GD coal and TDC.

Calculation of kinetic parameters

For the calculation of the activation energies, all heating rates have been used and they were estimated using the FR, FWO and DEAM methods. The values of activation energy of pyrolysis of coal blends with different addition of TDC obtained by FR, FWO and DAEM methods are shown in Tables 4, 5 and 6, respectively.

The mean values of activation energy calculated by the FR method were 478 kJ mol^{-1} , 333 kJ mol^{-1} , 351 kJ mol^{-1} , 329 kJ mol^{-1} and 291 kJ mol^{-1} for coal blends with 0 mass%, 10 mass%, 20 mass%, 30 mass% and 100 mass% TDC, respectively.

The mean values of activation energy calculated by the FWO method were 471 kJ mol^{-1} , 306 kJ mol^{-1} , 334 kJ mol^{-1} , 317 kJ mol^{-1} and 278 kJ mol^{-1} for coal blends with 0 mass%, 10 mass%, 20 mass%, 30 mass% and 100 mass% TDC, respectively.

The mean values of activation energy obtained by the DAEM method were 481 kJ mol^{-1} , 307 kJ mol^{-1} , 337 kJ mol^{-1} , 319 and 280 kJ mol^{-1} for coal blends with 0 mass%, 10 mass%, 20 mass%, 30 mass% and 100 mass% TDC, respectively.

Figure 7 shows the dependence of activation energy on conversion value, as calculated with FR, FWO and DAEM

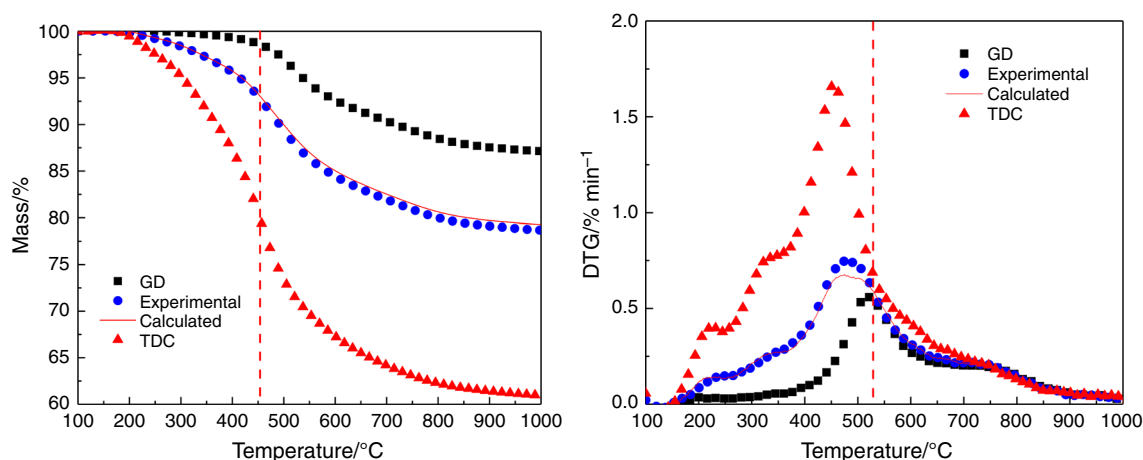


Fig. 6 Disparity between experimental and calculated TG and DTG curves of coal blends with 30 mass% TDC at the heating rate of 10 °C min⁻¹

Table 4 Activation energy of pyrolysis of coal blends with different addition of TDC obtained by FR method

Conversion	0 mass% TDC	10 mass% TDC	20 mass% TDC	30 mass% TDC	100 mass% TDC
0.2	375	206	231	230	156
0.3	379	242	261	249	203
0.4	426	259	271	253	228
0.5	523	295	289	276	261
0.6	575	317	339	303	282
0.7	555	407	417	371	342
0.8	458	406	490	488	369
0.9	530	530	510	459	490
Mean	478	333	351	329	291

Table 5 Activation energy of pyrolysis of coal blends with different addition of TDC obtained by FWO method

Conversion	0 mass% TDC	10 mass% TDC	20 mass% TDC	30 mass% TDC	100 mass% TDC
0.2	411	183	215	227	153
0.3	375	217	256	247	192
0.4	393	242	263	249	213
0.5	478	273	274	265	242
0.6	552	306	313	285	262
0.7	579	366	385	348	315
0.8	473	404	482	458	358
0.9	508	455	481	454	490
Mean	471	306	334	317	278

methods in the range of 0.2–0.9. The values of E obtained by three methods almost increased with increasing conversion, which indicates that the pyrolysis reaction becomes more difficult as it progresses. All results present almost the same tendency for coal blends with various addition of TDC.

Especially, it is evident that the values of the apparent activation energies obtained by FR method are higher than

the values of apparent activation energies obtained by FWO method. This is possible due to the fact that FR method which is a differential one uses the point value of the overall reaction rate, while FWO method which is an integral one describes the history of the system [26]. Therefore, the values of activation energy obtained by FWO method involve a systematic error that does not appear in the FR method. The FR method is more sensitive

Table 6 Activation energy of pyrolysis of coal blends with different addition of TDC obtained by DAEM method

Conversion	0 mass% TDC	10 mass% TDC	20 mass% TDC	30 mass% TDC	100 mass% TDC
0.2	419	180	214	228	150
0.3	382	215	257	248	191
0.4	400	242	264	249	212
0.5	489	274	275	266	243
0.6	566	307	316	286	263
0.7	593	370	390	352	318
0.8	481	408	491	466	363
0.9	516	460	489	460	500
Mean	481	307	337	319	280

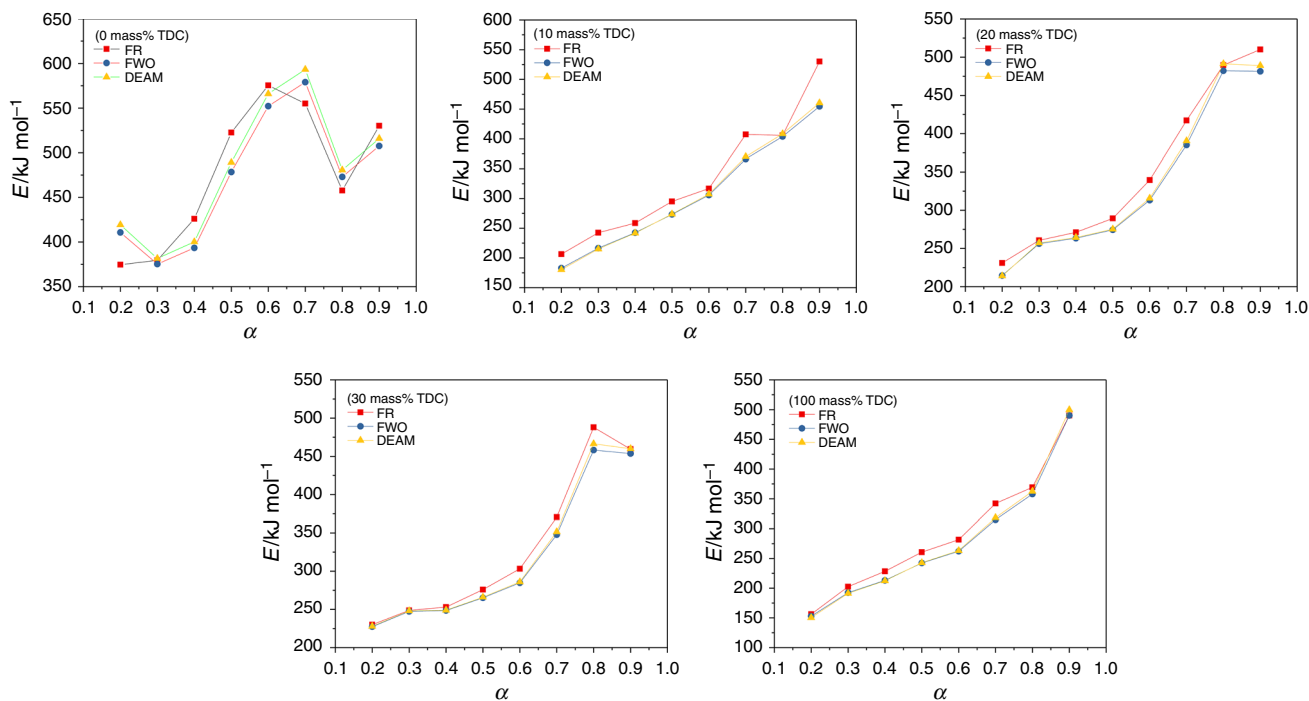


Fig. 7 Dependence of activation energy on the conversion for $\alpha = 0.2-0.9$ for coal blends with various addition of TDC

Table 7 Preexponential factor of pyrolysis of coal blends with different addition of TDC obtained by DAEM method

Conversion	0 mass% TDC	10 mass% TDC	20 mass% TDC	30 mass% TDC	100 mass% TDC
0.2	2.04E + 25	2.95E + 09	4.66E + 12	1.90E + 14	1.52E + 09
0.3	6.86E + 21	1.80E + 11	6.88E + 14	4.32E + 14	3.33E + 11
0.4	1.94E + 22	3.38E + 12	3.69E + 14	8.18E + 13	2.22E + 12
0.5	8.98E + 26	1.13E + 14	4.31E + 14	2.58E + 14	1.00E + 14
0.6	1.07E + 30	2.34E + 15	2.86E + 16	9.50E + 14	7.35E + 14
0.7	3.09E + 29	6.78E + 17	5.89E + 19	9.89E + 17	6.76E + 17
0.8	2.71E + 21	1.83E + 18	3.01E + 23	5.96E + 22	1.07E + 19
0.9	2.86E + 21	1.32E + 19	8.88E + 20	7.01E + 19	1.42E + 24
Mean	1.72E + 29	1.96E + 18	3.77E + 22	7.46E + 21	1.77E + 23

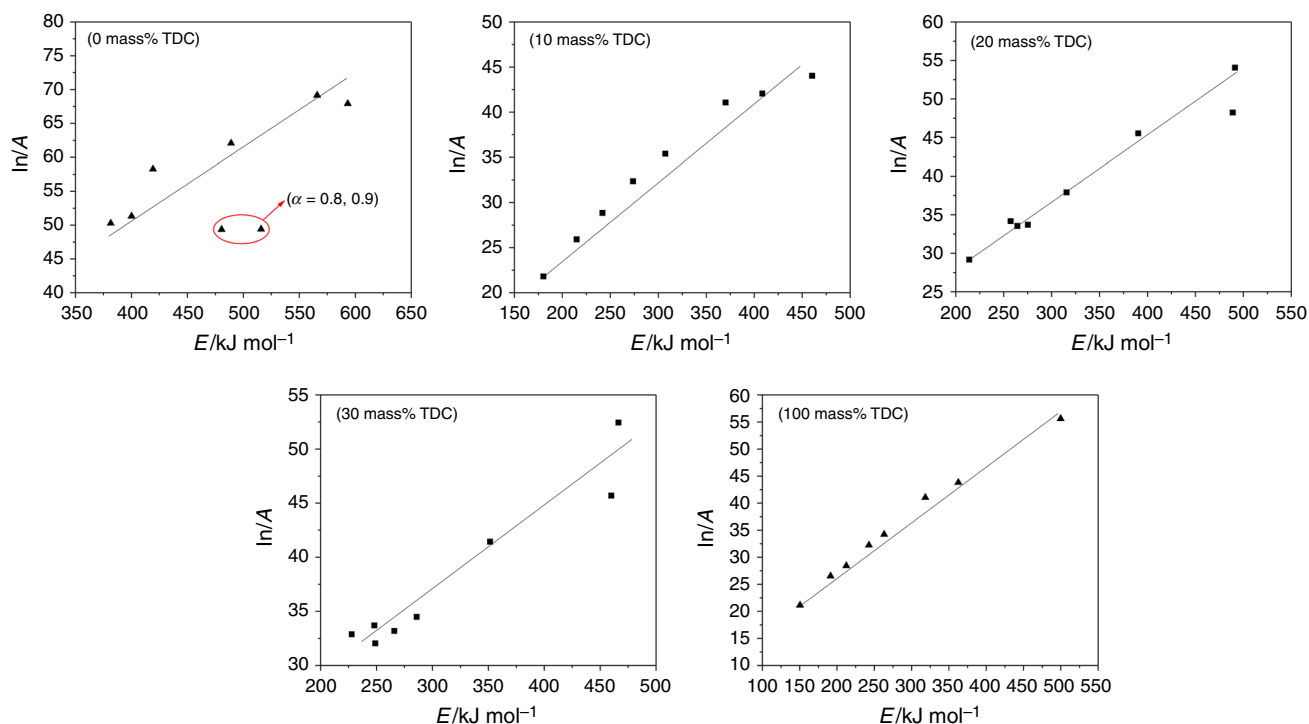


Fig. 8 Relationship between $\ln(A)$ and E determined for coal blends with various addition of TDC

than FWO method, and the values of activation energy obtained from the FR method are more reliable than those obtained from the FWO method [27].

For DAEM method, it can also be obtained the preexponential factor A , as Table 7 shown. The values of A obtained by DAEM method increased with increasing conversion. Therefore, there may be kinetic compensation effect in the kinetic process of coal pyrolysis. It is necessary to discuss in the next section.

Kinetic compensation effect

The kinetic compensation effect describes a lack of uniqueness in the determination of kinetic parameters of A and E . And its form can be described as follows

$$\ln A = \ln A_0 + aE \quad (11)$$

Figure 8 shows the relationship between $\ln(A)$ and E determined for coal blends with various addition of TDC. Through the slope and intercept of the above equation, the kinetic compensation effect equation of pyrolysis of different coal samples can be obtained. The reaction kinetics compensation effect equation of 0 mass% TDC with the conversion of α in the range of 0.2–0.7 was: $\ln A = 18.78 + 0.08643E$, the correlation coefficient $R^2 = 0.9234$. The points in the first diagram ($\alpha = 0.8$ and $\alpha = 0.9$) far from those of the fitting line. There may be two reasons to this weak correlation between $\ln A$ and E in the part of reaction kinetics compensation effect analysis.

Firstly, coal chemical structure has an important influence on kinetic parameters (such as preexponential factor A and activation energy E) [28].

Secondly, we can see that this range of conversion is in the late stage of pyrolysis which mainly occurs condensation of coal structure. There is a relatively high K content in the GD coal sample. And K in the coal has an important effect on structure of char during pyrolysis. In the late stage of pyrolysis ($\alpha = 0.8$ and $\alpha = 0.9$), the evaporation of K metal causes the coal structure to expand, resulting in a shift in the compensation effect. The reaction kinetics compensation effect equation of 10 mass% TDC with the conversion of α in the range of 0.2–0.9 was: $\ln A = 9.06 + 0.08096E$, the correlation coefficient $R^2 = 0.9639$. The reaction kinetics compensation effect equation of 20 mass% TDC with the conversion of α in the range of 0.2–0.9 was: $\ln A = 12.76 + 0.07942E$, the correlation coefficient $R^2 = 0.9591$. The reaction kinetics compensation effect equation of 30 mass% TDC with the conversion of α in the range of 0.2–0.9 was: $\ln A = 14.16 + 0.07538E$, the correlation coefficient $R^2 = 0.9326$. The reaction kinetics compensation effect equation of 100 mass% TDC with the conversion of α in the range of 0.2–0.9 was: $\ln A = 7.86 + 0.09827E$, the correlation coefficient $R^2 = 0.9901$. This indicates that the kinetic compensation effect does occur in the pyrolysis process of coal.

Conclusions

The pyrolysis of GD coal and TDC blends was investigated by non-isothermal thermogravimetric method. Experiments were performed with different coal samples (either individual samples or blends with different TDC content), at various heating rates. The results show that the pyrolysis start temperature of TDC is lower than that of GD coal, while the maximum devolatilization rate and the total volatile content of TDC are higher than those of GD coal. The effect of heating rate on the maximum rate of GD coal pyrolysis is greater than that on TDC pyrolysis. The addition of TDC not only improves the maximum devolatilization rate of coal blends, but also reduces the temperature corresponding to this maximum devolatilization rate. The TG and DTG curves of blends indicated that synergistic reactions may occur between the temperatures corresponding to the maximum devolatilization rates of GD coal and TDC. In this study, the apparent activation energy E obtained by FR, FWO and DAEM methods of coal blends with various addition of TDC almost increased with increasing conversion. There is a kinetic compensation effect in the kinetic process of coal pyrolysis and have got the reaction kinetics compensation effect equation. This study is helpful for the analysis of pyrolysis kinetics of TDC and associated blends.

Acknowledgements This work was supported by the National Natural Science Foundation of China (Grant No. 51574023).

References

- Zhang Y, Nakano J, Liu L, Wang X, Zhang Z. Co-combustion and emission characteristics of coal gangue and low-quality coal. *J Therm Anal Calorim.* 2015;120:1883–92.
- Chang J, Hu T, Liu X, Ren X. Construction of green infrastructure in coal-resource based city: a case study in Xuzhou urban area. *Int J Coal Sci Technol.* 2018;5:92–104.
- Liu BH, Zheng BN. Research on stagger arrangement mining method improving recovery ratio of coal resources. *Coal Technol.* 2018;37:101–3.
- Arenillas A, Rubiera F, Arias B, Pis JJ, Faúndez JM, Gordon AL, et al. A TG/DTA study on the effect of coal blending on ignition behaviour. *J Therm Anal Calorim.* 2004;76:603–14.
- Okuyama N, Komatsu N, Shigehisa T, Kaneko T, Tsuruya S. Hyper-coal process to produce the ash-free coal. *Fuel Process Technol.* 2004;85:947–67.
- Rahman M, Samanta A, Gupta R. Production and characterization of ash-free coal from low-rank Canadian coal by solvent extraction. *Fuel Process Technol.* 2013;115:88–98.
- Takanohashi T, Shishido T, Kawashima H, Saito I. Characterisation of HyperCoals from coals of various ranks. *Fuel.* 2008;87:592–8.
- Chang CM, Whang TJ, Huang DS, Wang DH, Tsai ST, Hung MT. Thermoplasticity and strength improvement of coking coal by addition of coal extracts. *Fuel.* 2014;117:364–71.
- Takanohashi T, Shishido T, Saito I. Effects of hypercoal addition on coke strength and thermoplasticity of coal blends. *Energy & Fuels.* 2008;22:1779–83.
- Casal MD, Canga CS, Díez MA, Alvarez R, Barriocanal C. Low-temperature pyrolysis of coals with different coking pressure characteristics. *J Anal Appl Pyrolysis.* 2005;74:96–103.
- Dong KS, Sang SP, Yong TK, Hwang J, Yu TU. Study of coal pyrolysis by thermo-gravimetric analysis (TGA) and concentration measurements of the evolved species. *J Anal Appl Pyrolysis.* 2011;92:209–16.
- Fermoso J, Arias B, Pevida C, Plaza MG, Rubiera F, Pis JJ. Kinetic models comparison for steam gasification of different nature fuel chars. *J Therm Anal Calorim.* 2008;91:779–86.
- Quan C, Xu S, An Y, Liu X. Co-pyrolysis of biomass and coal blend by TG and in a free fall reactor. *J Therm Anal Calorim.* 2014;117:817–23.
- Aboyade AO, Carrier M, Meyer EL, Knoetze JH, Görgens JF. Model fitting kinetic analysis and characterisation of the devolatilization of coal blends with corn and sugarcane residues. *Thermochim Acta.* 2012;530:95–106.
- Sarwar A, Khan MN, Azhar KF. Kinetic studies of pyrolysis and combustion of Thar coal by thermogravimetry and chemometric data analysis. *J Therm Anal Calorim.* 2012;109:97–103.
- Vyazovkin S, Wight CA. Model-free and model-fitting approaches to kinetic analysis of isothermal and nonisothermal data. *Thermochim Acta.* 1999;340–341:53–68.
- Bach QV, Tran KQ, Skreiberg Ø, Yan J. Combustion kinetics of wet-torrefied forest residues using the distributed activation energy model (DAEM). *Appl Energy.* 2017;185:1059–66.
- Parikh J, Channiwalla SA, Ghosal GK. A correlation for calculating HHV from proximate analysis of solid fuels. *Fuel.* 2005;84:487–94.
- Yang H, Chen H, Ju F, Yan R, Zhang S. Influence of pressure on coal pyrolysis and char gasification. *Energy Fuels.* 2007;21:3165–70.
- Du R, Wu K, Zhang L, She Y, Xu D, Chao C, et al. Thermal behavior and kinetic study on the pyrolysis of Shenfu coal by sectioning method. *J Therm Anal Calorim.* 2016;125:959–66.
- Zhang S, Zhu F, Bai C, Wen L, Zou C. Thermal behavior and kinetics of the pyrolysis of the coal used in the COREX process. *J Anal Appl Pyrolysis.* 2013;104:660–6.
- Cui HW, Jiu JT, Sugahara T, Nagao S, Sugauma K, Uchida H, et al. Using the Friedman method to study the thermal degradation kinetics of photonicallly cured electrically conductive adhesives. *J Therm Anal Calorim.* 2015;119:425–33.
- Aboulkas A, Harfi KE, Bouadili AE. Thermal degradation behaviors of polyethylene and polypropylene. Part I: Pyrolysis kinetics and mechanisms. *Energy Convers Manag.* 2010;51:1363–9.
- Han Y, Li T, Saito K. A modified Ortega method to evaluate the activation energies of solid state reactions. *J Therm Anal Calorim.* 2013;112:683–7.
- Caprariis BD, Santarelli ML, Scarsella M, Herce C, Verdone N, Filippis PD. Kinetic analysis of biomass pyrolysis using a double distributed activation energy model. *J Therm Anal Calorim.* 2015;121:1403–10.
- Çepeliogullar Ö, Pütün AE. Thermal and kinetic behaviors of biomass and plastic wastes in co-pyrolysis. *Energy Convers Manag.* 2013;75:263–70.
- Vyazovkin S. Modification of the integral isoconversional method to account for variation in the activation energy. *J Comput Chem.* 2001;22:178–83.
- Casal MD, Vega MF, Diaz-Faes E, Barriocanal C. The influence of chemical structure on the kinetics of coal pyrolysis. *Int J Coal Geol.* 2018;195:415–22.